Applied Catalysis B: Environmental 100 (2010) 289–298

Contents lists available at ScienceDirect

Applied Catalysis B: Environmental

journal homepage: www.elsevier.com/locate/apcatb

Kinetic modelling of TOC removal in the photocatalytic ozonation of diclofenac aqueous solutions

Fernando J. Beltrán*, Almudena Aguinaco, Juan F. García-Araya

Departamento de Ingeniería Química y Química Física, Universidad de Extremadura, 06006 Badajoz, Spain

ARTICLE INFO

Article history:
Received 27 April 2010
Received in revised form 2 August 2010
Accepted 5 August 2010
Available online 12 August 2010

Keywords:
Kinetic modelling
Diclofenac
Ozonation
Photocatalytic oxidation
Photocatalytic ozonation

ABSTRACT

A kinetic model for aqueous diclofenac photocatalytic ozonation is proposed and experimentally tested. The kinetic model, based on mol balance equations of main species present in water, gives total organic carbon (TOC), ozone and hydrogen peroxide concentrations with time as output variables. The model relies on both, experimental data obtained in this work (i.e. rate constant of reactions and quantum yield values) and published data on the nature of intermediate formation, free radicals and hydrogen peroxide yield and rate constants of the reactions between intermediates, ozone and hydroxyl radicals. Intermediates of different structure and reactivity towards ozone and hydroxyl radical have been classified into groups. Accordingly, the remaining TOC in water, at each time, is considered as the sum of the contributing TOC values of these groups. The kinetic model is applied to buffered systems and acceptably reproduces the experimental results for the reaction period investigated.

1. Introduction

Thousands of pharmaceutical compounds are currently approved for prescription and, as a result, a huge variety of these compounds and their metabolites are frequently found in many municipal wastewater treatment plants (WWTPs) [1,2]. Unit operations in WWTPs are in many cases unable to completely eliminate these substances and effluents are finally released to the water environment containing ng/L or even μg/L of these contaminants [3–5]. Because of the hazardous potential of these emergent contaminants (ECs) many works have been developed to find methods to eliminate them from water [6–8]. At present, advanced oxidation processes (AOPs), based on the formation and oxidising action of hydroxyl radicals, are considered as one of the most recommended technologies for this purpose [9,10].

Among AOPs, photocatalytic ozonation that combines the beneficial effect of ozone and photocatalytic oxidation, is subject of investigation at present. The most important advantage of this process is the removal of TOC from water as can be confirmed in recent publications [11,12]. Application of kinetic models to predicts TOC removal performance in AOPs can be a helpful tool. Although some works on AOP kinetic modelling have already been reported [13,14] literature still lacks of similar studies in the pharmaceutical photocatalytic ozonation involving the contribution of intermediate formation.

Among pharmaceutical compounds, diclofenac (DCF), a non-steroidal anti-inflammatory drug, is usually taken as model compound to study the effect of different processes (such as AOPs) for the removal of ECs. The reason is the frequent presence of this drug in municipal wastewaters [15,16] as a result of the worldwide use. The globally consumed volume of DCF is estimated to be 940 tons per year [17]. Thus, DCF removal from water or wastewater has been studied with the use of activated sludge and trickling filter beds [18], photocatalytic reactor membranes [19], ozonation alone and combined with hydrogen peroxide [20], UV C radiation [21], photocatalytic oxidation with UV lamps and solar light [22,23], UV/hydrogen peroxide oxidation [24,25] and ozone and activated carbon [26] to quote just a few works. Among these works ozonation processes are highly recommended because of the high DCF removal rates achieved although TOC reduction or kinetic studies are not usually reported.

In this work, a kinetic model of photocatalytic ozonation of DCF in water is presented based on a mechanism of reactions and rate data obtained here and/or reported in the literature. The kinetic model is checked by using experimental results obtained at different conditions.

2. Experimental

2.1. Materials and methods

Most of the information related to this section can be found in a previous paper [12]. DCF and t-butanol were obtained from Sigma–Aldrich and benzoquinone from Merck and used as received.

* Corresponding author. Tel.: +34 924289387; fax: +34 924289385.
E-mail address: fbeltran@unex.es (F.J. Beltrán).

0926-3373/$ – see front matter © 2010 Elsevier B.V. All rights reserved.
doi:10.1016/j.apcatb.2010.08.005

Ozone was generated in a laboratory ozone generator from pure oxygen. A commercial TiO_2 Degussa P25 (70% anatase and 30% rutile) was used as catalyst. DCF (30 ppm as average) aqueous solutions were buffered in ultrapure water (Millipore Q Millipore system) at pH 7 with NaH_2PO_4 and Na_2HPO_4 and ionic strength at 0.005 M.

Experiments were carried out in a 1 L capacity tubular borosilicate glass photoreactor (450 mm long, 80 mm diameter) described in a previous work [27]. About 0.9 L of an aqueous solution of DCF was charged into the reactor for each experiment. For the ozone based processes, an ozone–oxygen mixture was continuously bubbled into the solution throughout a diffuser placed at the bottom of the reactor. In some experiments, known amounts of t-butanol and benzoquinone were added to the DCF aqueous solution to discuss the role of radicals and oxidising holes in the photocatalytic process.

In photolytic experiments, the aqueous solution was irradiated with a high pressure mercury lamp (Heraeus, TQ 718 700 W) immersed in a glass well placed at the middle of the reactor. The efficient radiation of the lamp was only due to the 313 nm wavelength radiation as confirmed in a previous paper [28]. Then, hydrogen peroxide actinometry [29] was used to determine the intensity of the incident radiation that was found to be 3.42×10^{-5} Einstein s^{-1}. Additionally, the effective radiation path through the photoreactor was determined from low concentration hydrogen peroxide photolysis experiments following the procedure reported in a precedent work [30]. This parameter was found to be 8.2 cm.

For experiments involving TiO_2, the solid was kept in suspension by magnetic stirring with a concentration of 1.5 g L^{-1}. Steadily, samples were withdrawn from the reactor and analysed for parent compound and intermediate content, total organic carbon, hydrogen peroxide and ozone gas and dissolved ozone concentrations. Prior to the analysis, the solid was removed from samples by a 5415D Eppendorf Centrifuge and further filtration through a Millex-HA filter (Millipore, 0.45 μm).

2.2. Chemical analysis

DCF was analysed by high-performance liquid chromatography (Elite La Chrom) with a Sinergi 4 μm Hydro-RP 80 A column. A 80:20 (v/v) methanol–water mixture was used as mobile phase at a constant flow rate of 0.5 ml min^{-1}. For intermediates, a Supelcogel C-610 column was used. In this case, the mobile phase, at a flow rate of 0.75 ml min^{-1}, was ultrapure water. In addition, in all cases, the mobile phase was acidified at pH 2.5 with phosphoric acid (0.1% concentration). Detection was made with a L-2455 Hitachi Diode Array detector at 277 and 210 nm for DCF and carboxylic acid intermediates, respectively. Some of the intermediates (maleic, fumaric, oxalic, formic and malonic acids) were identified by comparing their retention times and absorbance spectrum in samples and standards.

Dissolved ozone concentration was measured by following the method proposed by Bader and Hoigné [31] based on the decoloration of the 5,5,7-indigotrisulphonate. Ozone in the gas phase was monitored by means of an *Anseros Ozomat* ozone analyser. The analysis was based on the absorbance at 254 nm. Hydrogen peroxide concentration was determined through the cobalt/bicarbonate method [32]. Total organic and inorganic carbon was monitored by a TOC-V_{SCH} Shimadzu carbon analyser.

3. Results and discussion

DCF is a compound that reacts very fast with ozone as previously reported in different papers [26,33–35]. Also, in a previous work DCF removal in the presence of ozone, UVA light and TiO_2, defined as photocatalytic ozonation, was studied and compared to single ozonation and photocatalytic oxidation [12]. These results and other experimentally obtained in this work are now considered to propose a kinetic model of the process. The kinetic model is based on mass balance equations of species participating in the reacting system (see Section 3.2.1). Solution of the kinetic model, however, first needs information concerning the kinetics of the reactions constituting the AOPs studied. The mechanism of reactions taking place can be built with the aid of literature [11,12,26,28,31–47] (see mechanism in supplementary part of this work). However, in order to confirm or eliminate the contribution of some reactions, a series of experiments of DCF photocatalytic oxidation with and without ozone were carried out in the presence of the so-called checking reactants such as t-butanol and benzoquinone.

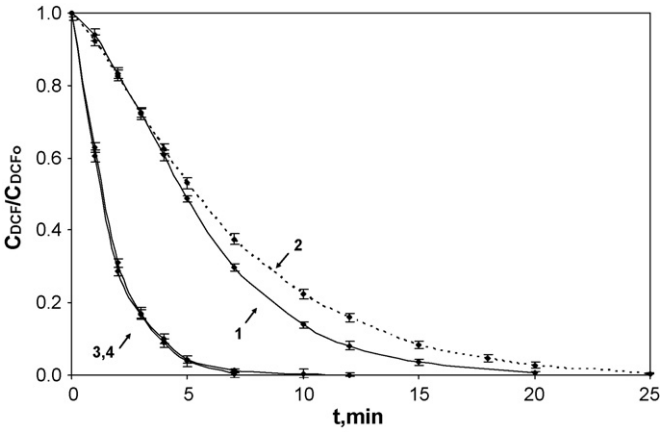

Fig. 1. Effect of t-butanol on the photocatalytic oxidation and photocatalytic ozonation of diclofenac in water. Conditions: C_{DCF} = 30 ppm, $C_{O_3 ge}$ = 10 mg/L, C_{TiO_2} = 1.5 g/L, gas flow rate: 30 L/h, pH = 7, T = 20 °C. Absence of t-butanol: 1: O_2/TiO_2/UVA; 3:O_3/TiO_2/UVA; presence of t-butanol: 2: O_2/TiO_2/UVA; 4: O_3/TiO_2/UVA.

3.1. Photocatalytic ozonation in the presence of checking reactants

As it is well known, t-butanol is frequently used as scavenger of hydroxyl radicals to check the development of advanced oxidation processes in the oxidising system studied. Here, some experiments of photocatalytic oxidation in the presence and absence of ozone and t-butanol were carried out for this purpose. The results are shown in Fig. 1. As it can be seen from Fig. 1, in the absence of ozone, after 3 min of reaction, t-butanol slows down the oxidation of DCF confirming the action of hydroxyl radicals in the UVA/TiO_2/O_2 system. A statistical 95% confidence test indicated the differences between these two experiments. When ozone is present, however, t-butanol seems to have no influence on DCF oxidation rate. Nevertheless, at the first minutes of reaction, DCF oxidation rate is slightly faster than in t-butanol absence. In this case, the statistical test showed no significant differences between experimental results. The results suggest that DCF is mainly consumed in its direct reaction with ozone although some contribution of hydroxyl radical oxidation cannot be disregarded. Since Sein et al. [34] reported the formation of ozonide ion radicals from the direct ozone-DCF reaction hydroxyl radical reactions should also develop. Also, the DCF direct photolysis can likely take place. According to the results shown in Fig. 1 and literature [34], the presence of t-butanol likely gives rise to two opposing effects. On one hand, t-butanol could reduce DCF oxidation rate by trapping the hydroxyl radicals generated from the ozone-DCF direct reaction and other free radical initiating reactions and, on the other hand, t-butanol, at the concentrations used in these experiments,

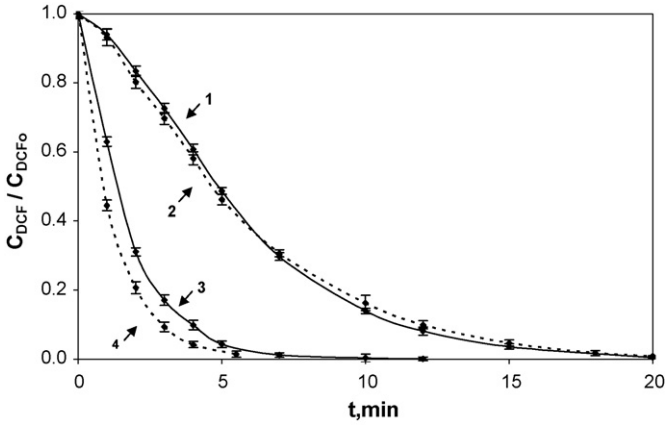

Fig. 2. Effect of benzoquinone on the photocatalytic oxidation and photocatalytic ozonation of diclofenac in water. Conditions as in Fig. 1. Absence of benzoquinone: (1) O_2/TiO_2/UVA; (3) O_3/TiO_2/UVA; presence of benzoquinone: (2) O_2/TiO_2/UVA; (4) O_3/TiO_2/UVA.

undoubtedly increase the specific interfacial area of gas bubbles leading to an increase of ozone mass transfer rate to water [48,49]. The latter effect would increase the DCF oxidation rate. Both opposing effects of t-butanol, as hydroxyl radical scavenger and ozone mass transfer enhancer, can be balanced so that DCF ozonation rate finally coincides in the presence and absence of t-butanol. Then, in the kinetic model that follows both direct (ozone and photolysis) reactions and hydroxyl radical contributions will be considered (see Section 3.2.1 for kinetic rate equations).

Benzoquinone is a substance usually taken as checking compound for superoxide ion radical oxidation [50]. In the photocatalytic oxidation system, one possible way of oxidation is through interaction between adsorbed superoxide ion radical and the organic matter (see reaction (ST19)). Benzoquinone would act in this system as free radical trapping. In the presence of ozone, however, the effect of benzoquinone cannot be tested since quinone aromatic compounds directly react very fast with ozone [51]. In any case, Fig. 2 shows the changes of DCF dimensionless concentration with time corresponding to these experiments. It can be observed from Fig. 2 that benzoquinone does not influence the DCF oxidation rate during photocatalytic oxidation, suggesting that superoxide ion radicals do not act as oxidising agent in this system, that is, reaction (ST19) can be neglected. On the contrary, when ozone is present, benzoquinone increases DCF oxidation rate. However, this rate increase is likely due to the formation of hydroxyl radicals from reactions (ST6) and (ST4), hydrogen peroxide being formed from the direct ozone-benzoquinone reaction. Then, in the presence of ozone, contribution of reaction (ST19) is negligible if compared to reaction (ST6). A statistical test conducted for these experiments confirms the conclusions drawn from Fig. 2.

3.2. Kinetic modelling

According to precedent comments and supplementary text, the mechanism of photocatalytic ozonation is reduced to reactions (ST1) to (ST16) and (ST23) to (ST27). In this work, the reactions were carried out in a semibatch agitated photoreactor where both the gas and water phases can be considered as perfectly mixed, that is, the concentration of any species is independent of the position and the ozone gas concentration at the reactor outlet is the same as in the gas inside the reactor. With the information gained through the flow type of gas and water phases and the mechanism of reactions proposed (see supplementary text), a rigorous kinetic model of DCF photocatalytic ozonation would require the establishment of mass balance equations of the species present in the reacting system, that is, DCF, ozone (in gas and water phases), hydrogen peroxide, intermediates and free radicals. However, only a few intermediates have been reported in the literature for the ozonation and photocatalytic oxidation of DCF [34,52,53] and no previous work has been done regarding photocatalytic ozonation intermediates. In this one, maleic, fumaric and oxalic acids have been identified. In addition, little is known about the sequence of reactions in the mechanism, that is, about the formation and removal of DCF and intermediates through their direct reactions with ozone and hydroxyl radicals, and, in some cases, through direct photolysis. For these reasons, the total organic carbon was taken as a surrogate parameter representing the organic matter present in water. Thus, in reactions (ST1), (ST7), (ST8), (ST23)–(ST25) TOC is considered instead of DCF and intermediates. However, given the different nature and reactivity of compounds formed during ozonation processes, TOC was first assumed as the sum of the contributions of two type of compounds: (a) TOC_1: formed by those compounds of high reactivity towards ozone, such as DCF itself, first intermediates of similar structure, one aromatic ring intermediates, and unsaturated carboxylic acids and (b) TOC_2: formed by compounds that exclusively react with hydroxyl radicals such as saturated carboxylic acids. The direct photolytic reaction was also assumed for TOC_1. Then, reactions considered were as follows:

With ozone:

$$3O_3 + TOC_1 \xrightarrow{k_{28}=7.2\times10^6\ M^{-1}\ s^{-1}} TOC_2 + 0.3O_3^{-\bullet} + 0.22H_2O_2 \quad (1)$$

With hydroxyl radicals

$$HO^\bullet + TOC_1 \xrightarrow{k_{29}=5\times10^9\ M^{-1}\ s^{-1}} TOC_2 + HO_2^\bullet \quad (2)$$

$$HO^\bullet + TOC_2 \xrightarrow{k_{30}=10^7\ M^{-1}\ s^{-1}} CO_2 + H_2O \quad (3)$$

With photons:

$$TOC_1 \xrightarrow{\lambda=313\ nm;\ I_0=3.42\times10^{-5}\ Einstein\ L^{-1}\ s^{-1}} TOC_2 \quad (4)$$

According to Sein et al. [34], in reaction (1), yields of 30% and 22% for the formation of the ozonide ion radical, O_3^-, and hydrogen peroxide, respectively, and a stoichiometric ratio of 3 mol ozone per mol TOC have been assumed. It should be reminded that at the conditions investigated one ozonide ion radical means one hydroxyl radical formed [41]. The rate constant value of reaction (1) was experimentally determined in this work.

Rate constant values assumed for hydroxyl free radical reactions with compounds constituting TOC_1 and TOC_2, have been taken from Buxton et al. [46]. In reaction (3) carbon dioxide formed was assumed to accumulate as bicarbonate ion.

For the photolytic reaction (4), the quantum yield (φ = 0.106 mol per photon) and absorptivity coefficient (ε = 65.3 $M^{-1}\ cm^{-1}$) values were the corresponding to DCF. These values were experimentally determined in this work following a procedure previously reported [28].

Terminations reactions occurred between TOC_2, phosphate and bicarbonate ions, considered in this work as inhibitors of ozone decomposition, with hydroxyl radicals:

$$H_2PO_4^- + HO^\bullet \xrightarrow{k_{32}=1.2\times10^7\ M^{-1}\ s^{-1}} H_2PO_4^\bullet + OH^- \quad (5)$$

$$HPO_4^{2-} + HO^\bullet \xrightarrow{k_{33}=8\times10^5\ M^{-1}\ s^{-1}} H_2PO_4^{-\bullet} + OH^- \quad (6)$$

$$HCO_3^- + HO^\bullet \xrightarrow{k_{34}=8.5\times10^6\ M^{-1}\ s^{-1}} CO_3^{-\bullet} + H_2O \quad (7)$$

The rate constants of reactions (5)–(7) were taken from Black and Hayon [54] and Weeks and Rabani [43]. Carbonate and phosphate ion radicals were considered as inactive.

3.2.1. Mass balance equations

Mass balances of the two TOCs assumed, ozone in the gas and water phases and hydrogen peroxide constituted the kinetic model. All of them correspond to the design equations for perfectly mixed reactors and are shown below:

For TOC_1:

$$-\frac{dTOC_1}{dt} = r_{D1} + r_{R1} + r_{UVA1} \quad (8)$$

where the three terms of the right side of Eq. (8) are the contributions of direct ozonation, free radical oxidation and direct photolysis to remove TOC_1 defined as follows:

$$r_{D1} = k_{28} C_{O_3} TOC_1 \quad (9)$$

$$r_{R1} = k_{29} C_{HOt} TOC_1 \quad (10)$$

$$r_{UVA1} = I_0 \phi_1 F_1 \left[1 - \exp(-2.303 L \sum_i \varepsilon_i C_i)\right] \quad (11)$$

with F_1 defined as the fraction of incident radiation that TOC_1 absorbs:

$$F_1 = \frac{\varepsilon_1 TOC_1}{\sum_i \varepsilon_i C_i} \quad (12)$$

and

$$\sum_i \varepsilon_i C_i = \varepsilon_1 TOC_1 + \varepsilon_{O_3} C_{O_3} + \varepsilon_H C_H \quad (13)$$

where ε is the absorptivity coefficient and subindexes 1, O_3 and H refer to TOC_1, ozone and hydrogen peroxide, respectively. Also, in Eqs. (10) and (11), C_{HOt}, I_0, L and φ_1 are the concentration of total hydroxyl radicals (sum of adsorbed and non-adsorbed hydroxyl radical concentrations), the intensity of incident radiation, the effective path of radiation through the photoreactor and the quantum yield of TOC_1 at 313 nm radiation (for data of these constants see Table ST-1 in the supplementary text).

For TOC_2:

$$\frac{dTOC_2}{dt} = r_{D1} + r_{R1} + r_{UV1} - r_{R2} \quad (14)$$

With

$$r_{R2} = k_{30} C_{OHt} TOC_2 \quad (15)$$

At any time:

$$TOC = TOC_1 + TOC_2 \quad (16)$$

For ozone in the gas phase:

$$(1-\beta)V\frac{dC_{O_3 g}}{dt} = v_g(C_{O_3 ge} - C_{O_3 g}) - k_L a\left(\frac{C_{O_3 g}RT}{He} - C_{O_3}\right)\beta V \quad (17)$$

where β, V, v_g, k_La, R, He, T and $C_{O_3 ge}$ are the liquid fraction, volume of reaction, gas flow rate, volumetric mass transfer coefficient, universal gas perfect and Henry constants, temperature and ozone gas concentration at the reactor inlet, respectively (see also Table ST1 for constant data).

For ozone in the water phase:

$$\frac{dC_{O_3}}{dt} = k_L a\left(\frac{C_{O_3 g}RT}{He} - C_{O_3}\right) - r_{O_3} - r_{UVO_3} \quad (18)$$

where r_{O_3} is the rate of ozone decomposition through reactions (1), (ST3), (ST4), (ST6), (ST9) and (ST26). The individual rate of any of these reactions is given by a second order kinetics:

$$r_i = k_i C_{O_3} C_i \quad (19)$$

where subindex i refers to the substance or free radical reacting with ozone according to the number of reaction. Also, r_{UVO_3} is the contribution of ozone direct photolysis at 313 nm, reaction (ST27), that presents a kinetic expression similar to the one of TOC_1 photolysis as shown in Eqs. (11)–(13). (For constant data see Table ST-1).

For hydrogen peroxide in water:

$$\frac{dC_H}{dt} = r_H \quad (20)$$

where r_H is the net formation rate of hydrogen peroxide:

$$r_H = 0.22 r_{D1} + r_{UVO_3} - k_4 C_{O_3} C_H \frac{10^{pH-pK_H}}{1+10^{pH-pK_H}} - k_H C_{OHt} C_H - r_{UVH} \quad (21)$$

with r_{UVH} as the contribution of direct photolysis at 313 nm that presents a kinetic expression similar to that of TOC_1 photolysis as shown in Eqs. (11)–(13) and

$$k_H C_H = (k_{11} + k_{12} 10^{pH-pK_H}) \frac{C_H}{1+10^{pH-pK_H}} \quad (22)$$

For carbon dioxide or, better, bicarbonate ion or inorganic carbon:

$$IC = TOC_0 - TOC \quad (23)$$

For free radicals, the steady state approximation was applied. Thus, for the superoxide ion radical the following equation applies:

$$k_{18} C_{Ti(III)} C_{O_2} + k_9 C_{O_3} C_{HOt} = k_6 C_{O_3} C_{O_2-} \quad (24)$$

This equation is, then, substituted in the ozone decomposition rate, Eq. (19). For the hydroxyl radical concentration it follows:

$$C_{OHt} = \frac{r_{in}}{k_t} \quad (25)$$

where r_{in} is the rate of initiation adding up the contributions from reactions (ST4), (ST21) and (1) to yield non-adsorbed hydroxyl radicals and reactions (ST16), (ST22) and (ST26) for adsorbed hydroxyl radicals:

$$r_i = 2k_4 C_{O_3}\left(\frac{10^{pH-pK_H}}{1+10^{pH-pK_H}} C_H\right) + 2r_{UVH} + 0.3 r_{D1} + k_{TiO_2} + (k_{22} C_H + k_{26} C_{O_3}) C_{Ti(III)} \quad (26)$$

and k_t being the scavenger factor, defined here as follows:

$$k_t = k_{30} TOC_2 + k_{32} C_{F1} + k_{33} C_{F2} + k_{34} C_{bic} \quad (27)$$

where C_{bic}, C_{F1} and C_{F2} are the concentrations of inorganic carbon or bicarbonate at pH 7 and the two species of phosphates present in solution at this pH, respectively.

Although literature provides values for most of the rate constants of the reactions in the kinetic model, some of them were determined in this work. Additionally, according to the mechanism proposed, the superoxide ion radical concentration can be expressed as a function of the hydroxyl radical concentration. Given the nature of the process, two types of hydroxyl radical were considered: adsorbed and non-adsorbed (see reactions (ST23) and (ST24) in supplementary text). The rate of initiation of adsorbed hydroxyl radicals depends, among other reactions, on the rate of positive hole formation, direct reaction (ST14). For these short life species, once the steady state approximation is applied to the corresponding mass balance, Eq. (28) is obtained:

$$\frac{dh^+}{dt} = k_{TiO_2} - k_2 C_{h+} - k_r C_{h+} C_{e-} = 0 \quad (28)$$

where k_{TiO_2} represents the rate of positive hole formation from the direct reaction (ST14) that, *a priori*, can be considered constant, provided the activity and stability of the semiconductor and intensity of effective incident radiation also remain constant during the process:

$$k_{TiO_2} = k C_{TiO_2}^n I_0^m = \text{constant} \quad (29)$$

I_0 is the intensity of the effective UVA radiation applied onto the catalyst surface and C_{TiO_2} the catalyst concentration. Also, in Eq. (28) the second and third terms of the right side represents the removal rates of positive holes through reactions (ST15) and (ST16) to form adsorbed hydroxyl radicals and the electron-hole recombination reaction or inverse reaction (ST14). The latter reaction, however, has been considered negligible due to the presence of electron trapping oxidant species such as oxygen, hydrogen peroxide and, specially, ozone (see reactions (ST17), (ST18), (ST19), (ST22) and (ST26)). Then, from Eq. (28), it can be stated:

$$k_{TiO_2} = k_2 C_{h+} = \text{rate of } OH_{ads} \text{ initiation} \quad (30)$$

A value of k_{TiO_2} was experimentally determined in this work from experiments of photocatalytic oxidation of oxalic acid. In this oxidising system, oxalic acid is only removed by reacting with hydroxyl radicals. Thus, the oxalic acid removal rate, in the semi-continous batch photoreactor used, is:

$$-\frac{dC_{Oxal}}{dt} = k_{HO} C_{Oxal} C_{HO_{ads}} = k_{HO} C_{Oxal} \frac{k_{TiO_2}}{k_t} = k_T C_{Oxal} \quad (31)$$

where k_{HO} and C_{Oxal} are the rate constant of the oxalic acid-adsorbed HO reaction and the concentration of oxalic acid, respectively, while k_t represents the scavenging factor [53], that is, the sum of the products between scavenger concentrations and corresponding rate constants of their reaction with hydroxyl radicals. In this work, phosphates (used to buffer at pH 7 the oxalic acid aqueous solution) played this role (see reactions (5) and (6)). Experimental results follow first order kinetics as Eq. (31) suggests (not shown). The least squares analysis of experimental points leads to the total rate constant, k_T, that was found to be $2.96 \times 10^4\ s^{-1}$. Since at the conditions applied the scavenging factor of phosphates is $k_t = 1.6 \times 10^5\ s^{-1}$ [26] k_{TiO_2} was calculated as $1.07 \times 10^6\ M^{-1}\ s^{-1}$. This rate constant was used in the kinetic model wherever the concentration of adsorbed hydroxyl radicals was used.

Before proceeding with the solution of the kinetic model, once all rate constants were known, two other considerations were made:

First: During the initial reaction time when DCF (and likely most TOC_1) was in solution [12] there is no much difference between TOC removal from ozone alone and photocatalytic ozonation experiments. Therefore, to validate the kinetic model, new experiments were conducted by first feeding ozone alone until total removal of DCF (about 5 min reaction) and then completed with the presence of TiO_2 and UVA radiation for the remaining reaction period to complete 120 min.

Second: Because of the relatively high initial DCF concentration, 10^{-4} M, the kinetic regime of ozone absorption was fast (Hatta number was higher than 3 [55]). Accordingly, dissolved ozone was not found during the first minutes of reactions (approximately the time needed to remove DCF [12], see also Fig. 5 later). Thus, as far as the kinetic model solution was concerned, during this initial period, a theoretical value of the ozone concentration in the water was calculated from the ozone mass balance equation by assuming that the accumulation rate of ozone was zero (see supplementary text for mass balance equations). In this way the kinetic model was solved until TOC_1 disappearance was observed. At that time, a slow kinetic regime was considered (in fact, the concentration of ozone calculated from the model at this time was in the range $4–6 \times 10^{-7}$ M) and the non-stationary regime first order differential equation corresponding to the mass balance of dissolved ozone and its reactions due to the presence of UVA radiation and catalyst were included in the kinetic model.

When the kinetic model was first solved, however, important differences were found between calculated and experimental results. Thus, calculated TOC values (sum of TOC_1 and TOC_2) were quite different than the experimental ones (not shown). Also, the kinetic model predicted an instantaneous appearance of hydrogen peroxide in opposition to the actual hydrogen peroxide concentration that reaches a maximum value after approximately 6 min of reaction. These discrepancies can be attributed to the different nature and ozone reactivity of intermediates. Thus, the rate constants of the reactions between ozone and both DCF and diclofenac-2-5-iminoquinone (DCF ozonation intermediate belonging to TOC_1, identified by Sein et al. [34]) vary nearly one order of magnitude while that of ozone-unsaturated carboxylic acids are two order of magnitude lower [40]. Also, the kinetic model predicts the formation of hydrogen peroxide just from the first reaction (1) when in fact, hydrogen peroxide is formed from aromatic ring opening or Criegge's mechanism (ozone addition to double carbon bonds), that is, ozone reactions with second or third DCF ozonation intermediates (see later). Then, it is evident that the kinetic model cannot be based on just one ozone–TOC and one HO–TOC reactions with one value for their corresponding rate constants.

3.2.2. Modified mechanism proposal

In order to correct and improve the kinetic model some new reactions were assumed. Thus, according to bibliography, the intermediates formed and eliminated from DCF oxidation can be re-classified to give five different TOC values, each of them showing different reactivity with ozone, and also, in some case, with hydroxyl radicals. Thus, these TOC contributions could be due to the following type of substances:

TOC_1 corresponding to the contribution of remaining DCF and first intermediates of similar reactivity toward ozone and hydroxyl radicals such as 5-hydroxy-diclofenac [34,53]. This corresponds to the following reactions:

$$TOC_1 + 3O_3 \xrightarrow{k_{39}=7.2\times10^6\ M^{-1}\ s^{-1}} 0.3O_3^{-\bullet} + TOC_2 \quad (32)$$

$$TOC_1 + HO^{\bullet} \xrightarrow{k_{40}=7.5\times10^9\ M^{-1}\ s^{-1}} 0.5TOC_2 + 0.5TOC_3 + HO_2\cdot \quad (33)$$

Reaction (32) is similar to reaction (1) but no hydrogen peroxide is considered to be formed. Reactions (32) and (33) have been contemplated following the results of Sein et al. [34] who observed a 30% (as estimate) yield of hydroxyl radical formation (which is formed from the ozonide ion radical) in the DCF-ozone reaction and two different intermediates (see below) from DCF hydroxyl radical oxidation. Also, as in reaction (1), the rate constant of reaction (32) corresponds to the value, experimentally determined in this work, for the DCF-ozone reaction at pH 7 following a procedure already published [28] and the stoichiometric ratio was reported by Sein et al. [34]. For the case of reaction (33) the rate constant also corresponds to the DCF-HO reaction as reported by Huber et al. [33]. In this case, two parallel reactions lead to compounds constituting TOC_2 and TOC_3 as deduced from the work of Sein et al. [34].

TOC_2 corresponding to the contribution of first intermediates of slightly lower reactivity with ozone, such as diclofenac-2-5-iminoquinone, identified by Sein et al. [34], who also reported a rate constant value for the reaction of this compound with ozone 5% of that of ozone-DCF reaction:

$$TOC_2 + O_3 \xrightarrow{k_{41}=3.6\times10^5\ M^{-1}\ s^{-1}} 0.3O_3^{-\bullet} + TOC_3 \quad (34)$$

$$TOC_2 + HO^{\bullet} \xrightarrow{k_{42}=5\times10^9\ M^{-1}\ s^{-1}} TOC_3 + HO_2^{\bullet} \quad (35)$$

In addition, for intermediates forming TOC_2 a general $5 \times 10^9\ M^{-1}\ s^{-1}$ value was assumed for the rate constant of reaction (35) [46].

TOC_3 corresponding to the contribution of following intermediates of reactivity slightly lower or similar to that of ozone-DCF reaction but constituted by aromatic ring compounds. Among these

intermediates, 2,6-dichloroaniline and/or 2-hydroxyphenylacetic acid have been reported [34,53]. The reactions are:

$$TOC_3 + O_3 \xrightarrow{k_{43}=5\times10^6\ M^{-1}\ s^{-1}} TOC_4 + 0.15H_2O_2 + 0.22O_3^{-\cdot} \quad (36)$$

$$TOC_3 + HO^{\bullet} \xrightarrow{k_{44}=5\times10^9\ M^{-1}\ s^{-1}} TOC_4 + HO_2^{\bullet} \quad (37)$$

For the direct reaction (36), the rate constant value has been taken as an average of the rate constants of reactions between ozone and compounds of similar nature (chlorinated anilines and substituted phenols, see [40,56]). Also, in reaction (36) 15 and 22% yields of hydrogen peroxide (due to ring opening) and ozonide ion radical, respectively, have been considered as reported by Mvula and von Sonntag [37] while studying the ozonolysis of phenols. Also, $5 \times 10^9\ M^{-1}\ s^{-1}$ was taken as the rate constant value for reaction (37) [46].

TOC_4 corresponding to the contribution of unsaturated carboxylic acids formed from ring opening in reactions (36) and (37). Compounds of this type have been identified in this work (maleic and fumaric acids). TOC_4 reactions are:

$$TOC_4 + O_3 \xrightarrow{k_{45}=10^4\ M^{-1}\ s^{-1}} TOC_5 + 0.65H_2O_2 \quad (38)$$

$$TOC_4 + HO^{\bullet} \xrightarrow{k_{46}=5\times10^9\ M^{-1}\ s^{-1}} TOC_5 + HO_2^{\bullet} \quad (39)$$

Rate constants of the ozone direct reactions with these compounds vary from 5×10^3 and $5 \times 10^4\ M^{-1}\ s^{-1}$ [39] so as a value of $10^4\ M^{-1}\ s^{-1}$ was taken. These reactions develop through the mechanism of Criegge yielding in one route hydrogen peroxide (65% yield was taken as an average from those reported by Leitzke and von Sonntag [39]) and carbon dioxide from a parallel route [39]. For this kinetic model 35% yield of carbon dioxide was then considered (see mass balance equations in supplementary text). Again, the rate constant of reaction (39) was taken as $5\times 10^9\ M^{-1}\ s^{-1}$ [46].

TOC_5, which is TOC_2 in the preceding failed kinetic model that corresponds to saturated carboxylic acids formed as final products before carbon dioxide. In this case, only reactions with hydroxyl radicals were considered:

$$TOC_5 + HO^{\bullet} \xrightarrow{k_{47}=10^7\ M^{-1}\ s^{-1}} CO_2 + H_2O \quad (40)$$

The rate constant of this reaction has been taken from the oxalic acid-OH radical reaction [57] (oxalic acid has been identified in this work). Contrary to what it is shown in reactions (33), (35), (37) and (39), from the TOC_5-HO reaction no hydroperoxide radical, $HO_2\cdot$, is assumed to be formed. As a consequence, TOC_5 constituting compounds can be considered as terminators of the radical chain, that is, true inhibitors of ozone decomposition. Again, all carbon dioxide formed was assumed to accumulate as bicarbonate ion. Termination reactions are also hydroxyl radical reactions with phosphate and bicarbonate ions (reactions (5)–(7)).

Finally, photolytic reactions were only considered for TOC_1 and TOC_2 since representative compounds (such as DCF) can be decomposed under the action of 313 nm radiation applied in this work. For the rest of TOC types, compounds such as phenol, anilines, unsaturated and saturated carboxylic acids do not show any absorption of light at this wavelength (as experimentally observed in this work). However, samples from AOPs experiments of some of these compounds (i.e. phenol, aniline), at the start of the process, showed a rather low absorbance at 313 nm (less than 0.02 absorbance units in a 1 cm length cell). As shown later (see Section 3.2.3) this light absorption did not represent any TOC variation when contribution of TOC_3 photolysis was included in the kinetic model. Thus, it should be reminded that the kinetic model predicts TOC variations with time and not changes of intermediate concentrations. Also, TOC conversion achieved during DCF UVA radiation experiments made in this work was lower than 10% after 120 min reaction with the maximum TOC elimination rate achieved during the first minutes (likely due to TOC_1 and TOC_2 forming compounds). Then, although some unknown intermediates contributing to TOC_3 could undergo photolysis at 313 nm radiation, this photoreaction would likely yield other intermediates rather than any TOC reduction. Therefore, no contribution of direct photolysis was considered for TOC_3. Photolysis reactions are then:

$$TOC_1 \xrightarrow{\lambda=313\ nm;\ I_0=3.42\times10^{-5}\ Einstein\ L^{-1}\ s^{-1}} TOC_2 \quad (41)$$

$$TOC_2 \xrightarrow{\lambda=313\ nm;\ I_0=3.42\times10^{-5}\ Einstein\ L^{-1}\ s^{-1}} TOC_3 \quad (42)$$

Absorptivity coefficients and quantum yields values for TOC_1 and TOC_2 were those of DCF photolysis.

3.2.3. Checking the kinetic model

Once the kinetic model was applied and deviations were observed, some modifications were introduced. These modifications affected to the constituents of TOC that now will be the sum of five contributions as indicated in the previous section. Reactions considered now in the mechanism are: (ST2) to (ST18), (ST26) and (ST27), (5)–(7) and (32)–(42). This affected the mass balance equations as follows:

For TOC_1:

$$-\frac{dTOC_1}{dt} = r_{D1} + r_{R1} + r_{UVA1} \quad (43)$$

where:

$$r_{D1} = k_{39}C_{O_3}TOC_1 \quad (44)$$

$$r_{R1} = k_{40}C_{HOt}TOC_1 \quad (45)$$

$$r_{UVA1} = I_0\phi_1F_1\left[1 - \exp(-2.303L\sum\nolimits_i \varepsilon_i C_i)\right] \quad (46)$$

with parameters of Eq. (46) as indicated in Eq. (11).

For TOC_2:

$$\frac{dTOC_2}{dt} = 0.5r_{D1} + r_{R1} + r_{UV1} - (r_{D2} + r_{R2} + r_{UV2}) \quad (47)$$

with rate expressions for r_{D2}, r_{R2} and r_{UV2} similar to those of Eqs. (9)–(11), respectively, but including rate constants of reactions (35) and (36) of the previous section. Parameters present in r_{UV2} are considered the same as in r_{UV1}.

For TOC_3:

$$\frac{dTOC_3}{dt} = r_{D21} + r_{R2} + r_{UV2} - (r_{D3} + r_{R3}) \quad (48)$$

where rate expressions for r_{D3} and r_{R3} are similar to those for TOC_2 but including the rate constants of reactions (36) and (37), respectively.

For TOC_4:

$$\frac{dTOC_4}{dt} = r_{D3} + r_{R3} - (r_{D4} + r_{R4}) \quad (49)$$

where rate expressions for r_{D4} and r_{R4} are similar to those of TOC_3 but including the rate constants of reactions (38) and (39), respectively.

For TOC_5:

$$\frac{dTOC_5}{dt} = r_{D4} + r_{R4} - r_{R5} \quad (50)$$

where rate expression for r_{R5} is similar to the other rate expressions for hydroxyl radical-compound reactions, including now the rate constant of reaction (40).

For ozone in the gas and in the water phases, Eqs. (17) and (18), respectively, are again used. However, r_{O_3} in Eq. (18), is the rate of ozone decomposition through reactions (32), (34), (36), (38), (ST3),

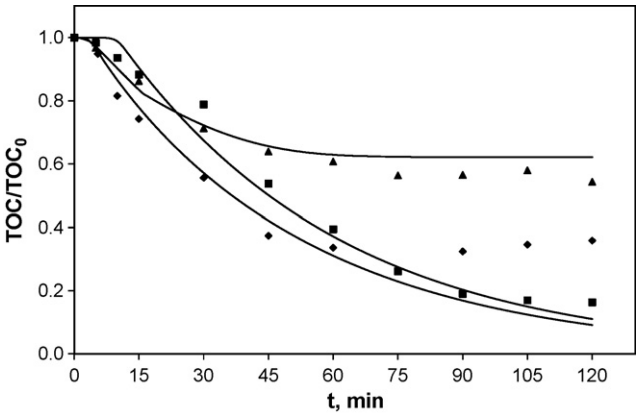

Fig. 3. Experimental (symbols) and calculated (curves) TOC with time for different diclofenac oxidation systems applied. Conditions as in Fig. 1. ■: O_2/TiO_2/UVA; ♦: O_3/TiO_2/UVA; ▲: O_3 (with $k_{48} = 5 \times 10^7\ M^{-1}\ s^{-1}$).

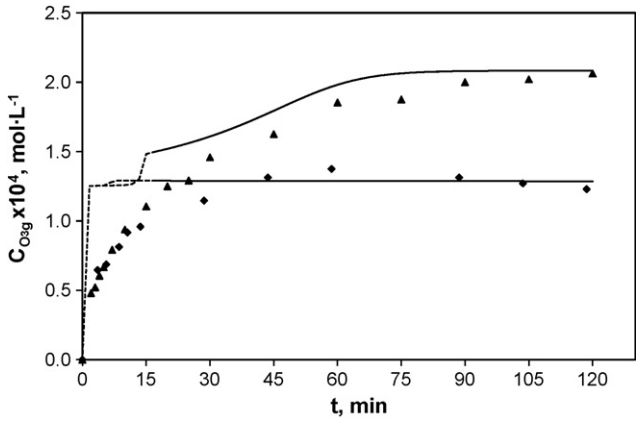

Fig. 4. Experimental (symbols) and calculated (curves) of the concentration of ozone in the gas leaving the reactor with time for diclofenac ozonation alone and diclofenac photocatalytic ozonation. Conditions as in Fig. 1. ♦: O_2/TiO_2/UVA ▲: O_3 (with $k_{48} = 5 \times 10^7\ M^{-1}\ s^{-1}$). Dotted points correspond to the initial reaction period where dissolved ozone concentration is obtained from Eq. (18) with the ozone accumulation rate, $dC_{O_3}/dt = 0$ due to fast kinetic regime of ozone absorption.

(ST4), (ST6), (ST9), (ST26) and (ST27). The individual rate of any of these reactions is given by a second order kinetics.

For hydrogen peroxide in water, also, Eq. (20) is applied, but r_H, the net formation rate of hydrogen peroxide, is now:

$$r_H = 0.15r_{D3} + 0.65r_{D4} + r_{UVO_3} - k_4 C_{O_3} C_H \frac{10^{pH-pK_H}}{1+10^{pH-pK_H}} - k_H C_{OHt} C_H - r_{UVH} \quad (51)$$

For bicarbonate ion, Eq. (23) still applies.

For free radicals, the steady state approximation was applied and Eq. (24) for the superoxide ion radical and (25) for hydroxyl radicals still hold although the initiation rate of these free radicals is now the contributions of reactions (ST4), (ST21) and (1) to yield non-adsorbed hydroxyl radicals and reactions (ST16), (ST22) and (ST26) for adsorbed hydroxyl radicals:

$$r_i = 2k_4 C_{O_3}\left(\frac{10^{pH-pK_H}}{1+10^{pH-pK_H}} C_H\right) + 2r_{UVH} + 0.3(r_{D1}+r_{D2}) + 22r_{D3} + k_{TiO_2} + (k_{22}C_H + k_{26}C_{O_3})C_{Ti(III)} \quad (52)$$

Finally, k_t, the scavenger factor, is defined as in Eq. (27):

$$k_t = k_{48}TOC_5 + k_{32}C_{F1} + k_{33}C_{F2} + k_{34}C_{bic} \quad (53)$$

With the modified kinetic model, the same considerations made previously regarding the initial reaction period were applied. Therefore, the change of kinetic regime was taken, as before, once the calculated dissolved ozone concentration was about 4×10^{-7} M (approximately first 5 min of reaction). At this reaction time TOC_1 to TOC_3 have disappeared and approximately 70% of maximum calculated TOC_4 was still present (see Fig. 6). Due to the high ozone reactivity of compounds constituting TOC_1 to TOC_3 and, in a lesser extent, TOC_4 a fast kinetic regime of ozonation would be expected during these first minutes of reactions which supports the procedure applied [55].

Figs. 3–6 show the calculated and experimental values of TOC (as a sum of all TOC contributions) and concentrations of ozone (in the gas leaving the reactor and in the water) and hydrogen peroxide, respectively, with time for one photocatalytic ozonation experiment (also, in some cases, experimental and calculated results for ozonation alone and photocatalytic oxidation runs are presented). In all cases the goodness of fit was determined by calculating the

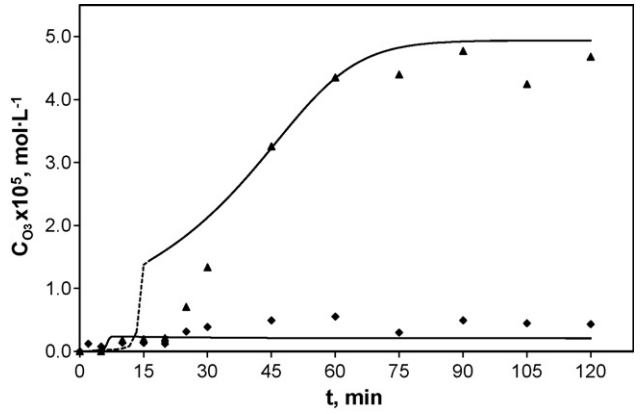

Fig. 5. Experimental (symbols) and calculated (curves) of the concentration of dissolved ozone with time for diclofenac ozonation alone and diclofenac photocatalytic ozonation. Conditions as in Fig. 1. ♦:O_2/TiO_2/UVA ▲: O_3 (with $k_{48} = 5 \times 10^7\ M^{-1}\ s^{-1}$). Dotted points correspond to the initial reaction period where dissolved ozone concentration is obtained from Eq. (18) with the ozone accumulation rate, $dC_{O_3}/dt = 0$ due to fast kinetic regime of ozone absorption.

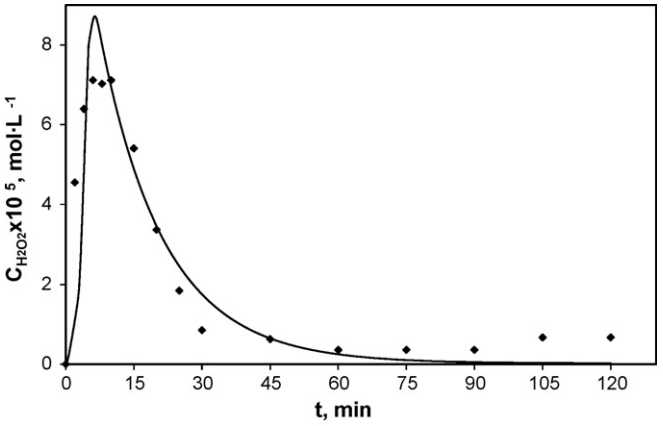

Fig. 6. Experimental (symbols) and calculated (curves) of the concentration of hydrogen peroxide with time for diclofenac photocatalytic ozonation. Conditions as in Fig. 1.

Theil's inequality coefficient, TIC, defined as follows [58]:

$$TIC = \frac{\sqrt{\sum_i (y_{c,i} - y_{e,i})^2}}{\sqrt{\sum_i y_{c,i}^2} + \sqrt{\sum_i y_{e,i}^2}} \quad (54)$$

A value of TIC lower than 0.3 indicates a good agreement between experimental ($y_{e,i}$) and calculated, ($y_{c,i}$), results. Once applied Eq. (54) to the results of the kinetic model the condition of good agreement was always achieved, except in some case for data corresponding to advanced reaction times (see Fig. 3).

In Fig. 3 the changes of total experimental TOC and calculated TOC as the sum of TOC_1 to TOC_5 contributions with time are displayed. Also, results of DCF buffered ozonation and photocatalytic oxidation experiments are shown. Regarding photocatalytic ozonation, as can be seen from Fig. 3, the calculated results follow the experimental data with high concordance during the first minutes of reaction (when non-photocatalytic ozonation was applied), where a short induction period is observed, and for the first hour of reaction. After this reaction time, actual TOC removal rate is stopped and the kinetic model underestimates the experimental results. It is speculated that after this reaction time TiO_2 activity rapidly decays as a result of ozone and phosphate presence. This conclusion is based, on one hand, on the results obtained in unbuffered photocatalytic ozonation experiments and, on the other hand, on buffered photocatalytic oxidation experiments where the TOC removal inhibition period is not observed [12]. Unfortunately, unbuffered photocatalytic ozonation experiments could not be simulated due to the pH decrease (approximately 1.5 units) that would imply consideration of unknown pKs of dissociated compounds formed (phenolics, carboxylic acids, etc.) to simulate pH changes that also lead to ozone direct rate constant changes for the ozone-dissociating compound reactions. Results of TOC with time for different conditions of initial TOC (derived from the initial DCF concentration applied) and ozone concentration in the gas fed to the reactor show similar concordance to those of Fig. 3 between experimental and calculated results. The kinetic model was also used to check any contribution of TOC_3 intermediate photolysis to TOC elimination. Thus, in the mass balance equation for TOC_3, Eq. (48), contribution of photolysis rate (with the absorptivity coefficient and quantum yield of TOC_1) was included and the kinetic model solved. Comparing these results with those shown in Fig. 3 no differences at all were observed in the variation of TOC with time, which supports the experimental results about the very low TOC changes observed during DCF photolysis after the first minutes of reaction.

Fig. 4 presents the results corresponding to the ozone gas concentration profiles at the reactor outlet. In this case, however, the kinetic model does not provide accurate calculated results for the initial reaction period (the first 5 min of reaction) because of the approximate way of determining the dissolved ozone concentration. This leads to gas phase ozone concentration values higher than expected for this reaction period (see dotted points in Fig. 4). After this initial period a good concordance is found between experimental and calculated ozone gas concentrations.

Fig. 5 gives the experimental and calculated concentrations of the dissolved ozone concentration with time for the experiment of Fig. 3. As can be observed from Fig. 5 the kinetic model also leads to acceptable results. In this case, it is highlighted the absence of ozone during the first minutes of ozonation, regardless of the ozone process, due to the fast kinetic regime of ozonation.

To account for all of the main species in the system, in Fig. 6 the experimental and calculated results of hydrogen peroxide concentration with time are plotted for the case of the photocatalytic ozonation experiment. It is seen from Fig. 6 that the kinetic model does not only properly simulate the experimental results but also

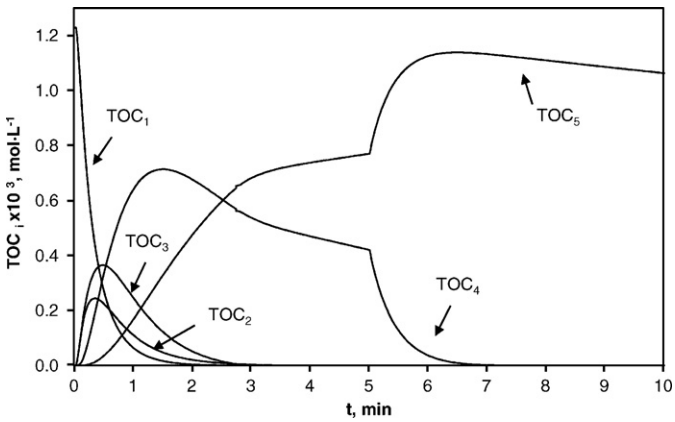

Fig. 7. Changes of theoretical assumed TOC contributions (TOC_1 to TOC_5) with time for the kinetic model of diclofenac photocatalytic ozonation. Conditions as in Fig. 1.

the time where the maximum concentration of hydrogen peroxide is reached. This supports the assumptions made on the type of TOC which, by reacting with ozone, acted as a main source of hydrogen peroxide formation, that is TOC_3 and TOC_4, corresponding to single aromatic and unsaturated carboxylic acid intermediates. In fact, when only two TOC types were considered the kinetic model predicted an erroneous instantaneous hydrogen peroxide formation.

Finally, in Fig. 7 the changes of different assumed TOCs with time are presented. As it can be seen, TOC_1 rapidly decreases with time due to the ozonation alone process while the rest of TOC profiles behave as expected in a series-parallel reacting system. The kinetic model, however, predicts a TOC_1 removal rate faster than that expected from DCF removal rate (not shown) which likely indicates that more intermediate TOCs should be assumed to fit these data although total TOC results would be unaffected (see Fig. 3). It can also be noticed the sudden increase of TOC_4 removal rate observed just when TiO_2 and UVA radiation were considered in the kinetic modelling, that is, when approximately the ozonation kinetic regime changed from fast to slow. At this time, the model predicts the absence of compounds constituting TOC_1 to TOC_3 and ozone reactions in the slow kinetic regime.

Since the kinetic model involves reactions of ozone and photocatalytic oxidation processes, the experimental results of these two oxidising systems should also be modelled. Thus, in the following sections some results are discussed about these possible applications.

3.3. *The kinetic model for the non-photocatalytic ozonation process*

Non-photocatalytic ozonation and the ozone alone process were also simulated with the kinetic model. Thus, reactions corresponding to photocatalytic oxidation were not considered. Some comparison results are shown in Figs. 3–5. For this oxidising system, the same rules concerning the kinetic regime of ozone absorption applied. Calculated TOC results overestimated the experimental ones, especially during the longer period of slow kinetic regime (not shown). During this period main reactions are those between hydroxyl radicals and refractory compounds such as oxalic acid. The kinetic model, however, gives good TOC predictions when the rate constant of reaction (40) was increased 5 times (see Fig. 3). One possible explanation of these results can be due to the nature of TOC_5 forming compounds. It is likely that these compounds are not exactly the same as in the photocatalytic ozone process so that the rate constant of their reaction with the hydroxyl radical could be higher. If the five times increase of this rate constant is considered the kinetic model perfectly simulated the experimental results of

TOC and ozone in the gas and water as shown in Figs. 4 and 5. No measurements were made for hydrogen peroxide concentration in this case.

3.4. The kinetic model for the photocatalytic oxidation process

Also, the kinetic model was applied for the photocatalytic oxidation process with the results also shown in Figs. 3–5. As far as TOC results are concerned the kinetic model predicted TOC removal rates much faster than the experimental ones (not shown). However, these anomalous results have a logical explanation since the kinetic model only considers reaction (40) as the main step to form bicarbonate, one of the hydroxyl radical inhibitors. For the photocatalytic oxidation system, it is reasonable to admit that other HO-TOC reactions also form part of the scavenger effect of the system (see k_t in Eq. (31)) since they produce the hydroperoxide radical (or superoxide ion radical, see equilibrium (ST5)) that, in the absence of ozone, does not regenerate the hydroxyl radical through reaction (ST6). Notice that one ozonide ion radical instantaneously gives one hydroxyl radical at the conditions applied [41]. Then, the kinetic model leads to good TOC results if a 15% of the sum of TOC_1 to TOC_4, in addition to TOC_5 as the model already applied, is considered as scavenger of hydroxyl radical. For this case, the scavenging factor is given by Eq. (55):

$$k_t = 0.15\,(k_{40}\mathrm{TOC}_1 + k_{43}\mathrm{TOC}_2 + k_{45}\mathrm{TOC}_3 + k_{47}\mathrm{TOC}_4) + k_{48}\mathrm{TOC}_5 + k_{32}C_{F1} + k_{33}C_{F2} + k_{34}C_{bic} \quad (55)$$

In buffered systems after approximately 60 min of reaction, experimental photocatalytic oxidation leads to higher TOC removal than experimental photocatalytic ozonation (see Fig. 3). However, during the first hour of reaction TOC oxidation rate is faster when ozone is applied. In non-buffering systems, photocatalytic ozonation is the process leading to the highest TOC conversion regardless of reaction time [12].

4. Conclusions

Main conclusions of this work are:

The rate constant of photocatalytic oxidation of DCF has been estimated to be $1.07 \times 10^6\ M^{-1}\ s^{-1}$. This value likely remains constant for the first 60 min of photocatalytic ozonation. From this reaction time, a decrease of catalyst activity is predicted.

The rate constant value of the ozone-DCF reaction has been calculated to be $7.2 \times 10^6\ M^{-1}\ s^{-1}$.

The quantum yield of DCF photolysis at 313 nm was determined to be 0.106 mol photon^{-1}.

TOC based kinetic models of photocatalytic ozonation reactions can be established from experimental data obtained in this work and already published on the nature, formation yields of intermediates, reaction rate constants of their reactions with ozone and hydroxyl radical and quantum yields of direct photolysis. However, the kinetic model presented in this work is only valid for phosphate buffering systems where pH is kept constant. Then, these kinetic models should be completed for unbuffering systems where pH changes. This implies more information related to pK of dissociating intermediates formed and, even, with the kinetics and equilibrium adsorption steps in the case compounds also adsorb on the catalyst surface. Considerations of this type are now been followed and will be the subject of future work.

Acknowledgments

The authors acknowledge the economic support of MICINN of Spain and European Feder Funds through Projects CTQ2006/04745 and CTQ2009/13459-C05-05. Also, Mss Almudena Aguinaco thanks the Spanish Ministry of Education for providing her a FPU grant.

Appendix A. Supplementary data

Supplementary data associated with this article can be found, in the online version, at doi:10.1016/j.apcatb.2010.08.005.

References

[1] J.L. Santos, I. Aparicio, M. Callejón, E. Alonso, J. Hazard. Mater. 164 (2009) 1509–1516.
[2] C. Yu, K. Chu, Chemosphere 75 (2009) 1281–1286.
[3] A.J. Watkinson, E.J. Murby, S.D. Costanzo, Water Res. 41 (2007) 4146–4176.
[4] N. Vieno, T. Tuhkanen, L. Kronberg, Water Res. 41 (2007) 1001–1012.
[5] A.Y. Lin, T. Yu, S.K. Lateef, J. Hazard. Mater. 167 (2009) 1163–1169.
[6] N. Nakada, H. Shinohara, A. Murata, K. Kiri, S. Managaki, N. Sato, H. Takada, Water Res. 41 (2007) 4373–4382.
[7] S.D. Kim, J. Cho, I.S. Kim, B.J. Vanderford, S.A. Snyder, Water Res. 41 (2007) 1013–1021.
[8] W. Hua, E.R. Bennett, R.J. Letcher, Water Res. 40 (2006) 2259–2266.
[9] S. Esplugas, D.M. Bila, L. Gustavo, T. Krause, M. Dezotti, J. Hazard. Mater. 149 (2007) 631–642.
[10] L. Yang, C. Hu, Y. Nie, J. Qu, Environ. Sci. Technol. 43 (2009) 2525–2529.
[11] F.J. Beltrán, A. Aguinaco, J.F. García-Araya, A. Oropesa, Water Res. 42 (2008) 3799–3808.
[12] J.F. García-Araya, F.J. Beltrán, A. Aguinaco, J. Chem. Technol. Biotechnol. 85 (2010) 798–804.
[13] F.J. Rivas, F.J. Beltrán, O. Gimeno, M. Carbajo, Ind. Eng. Chem. Res. 45 (2006) 166–174.
[14] M. Addamo, V. Augugliaro, E. Garcia-Lopez, V. Loddo, G. Marcí, L. Palmisano, Catal. Today 107–108 (2005) 612–618.
[15] B. Kasprzyk-Hordern, R.M. Dinsdale, A.J. Guwy, Water Res. 42 (2008) 3498–3518.
[16] J.L. Zhou, Z.L. Zhang, E. Banks, D. Grover, J.Q. Jiang, J. Hazard. Mater. 166 (2009) 655–661.
[17] Y. Zhang, S. Geißen, C. Gal, Chemosphere 73 (2008) 1151–1161.
[18] B. Kasprzyk-Hordern, R.M. Dinsdale, A.J. Guwy, Water Res. 43 (2009) 363–380.
[19] M.J. Benotti, B.D. Stanford, E.C. Wert, S.A. Snyder, Water Res. 43 (2009) 1513–1522.
[20] R. Rosal, A. Rodríguez, J.A. Perdigón-Melón, M. Mezcua, M.D. Hernando, P. Letón, E. García-Calvo, A. Agüera, A.R. Fernández-Alba, Water Res. 42 (2008) 3719–3728.
[21] S. Canonica, L. Meunier, U. von Gunten, Water Res. 42 (2008) 121–128.
[22] L. Rizzo, S. Meric, D. Kassinos, M. Guida, F. Russo, V. Belgiorno, Water Res. 43 (2009) 979–988.
[23] F. Méndez-Arriaga, S. Esplugas, J. Jiménez, Water Res. 42 (2008) 585–594.
[24] D. Vogna, R. Marotta, A. Napolitano, R. Andreozzi, M. d'Ischia, Water Res. 38 (2004) 414–422.
[25] I. Kim, N. Yamashita, H. Tanaka, J. Hazard. Mater. 166 (2009) 1134–1140.
[26] F.J. Beltrán, P. Pocostales, P. Alvarez, A. Oropesa, J. Hazard. Mater. 163 (2009) 768–776.
[27] F.J. Beltrán, O. Gimeno, F.J. Rivas, M. Carbajo, J. Chem. Technol. Biotechnol. 81 (2006) 1787–1796.
[28] F.J. Beltrán, A. Aguinaco, J.F. García-Araya, Water Res. 43 (2009) 1359–1369.
[29] I. Nicole, J. DeLaat, M. Doré, J.P. Duguet, C. Bonnel, Water Res. 24 (1990) 157–168.
[30] F.J. Beltrán, G. Ovejero, J.F. García-Araya, F.J. Rivas, Ind. Eng. Chem. Res. 34 (1995) 1607–1615.
[31] H. Bader, J. Hoigné, Water Res. 15 (1981) 449–456.
[32] W. Masschelein, M. Denis, R. Ledent, Water Sewage Works August (1977) 69–72.
[33] M.M. Huber, S. Canonica, G.Y. Park, U. von Gunten, Environ. Sci. Technol. 37 (2003) 1016–1024.
[34] M.M. Sein, M. Zedda, J. Tuerk, T.C. Schmidt, A. Golloch, C. von Sonntag, Environ. Sci. Technol. 42 (2008) 6656–6662.
[35] A.D. Coelho, C. Sans, A. Agüera, M.J. Gómez, S. Esplugas, M. Dezotti, Sci. Total Environ. 407 (2009) 3572–3578.
[36] T.E. Agustina, H.M. Ang, V.K. Vareek, J. Photochem. Photobiol. C: Photochem. Rev. 6 (2005) 264–273.
[37] E. Mvula, C. von Sonntag, Org. Biomol. Chem. 1 (2003) 1749–1756.
[38] M. Buffle, U. von Gunten, Environ. Sci. Technol. 40 (2006) 3057–3063.
[39] A. Leitzke, C. von Sonntag, Ozone Sci. Eng. 31 (2009) 301–308.
[40] J. Hoigné, H. Bader, Water Res. 17 (1983) 185–194.
[41] S. Staehelin, J. Hoigné, Environ. Sci. Technol. 19 (1985) 1206–1212.
[42] S. Staehelin, J. Hoigné, Environ. Sci. Technol. 16 (1982) 666–681.
[43] J.L. Weeks, J. Rabani, J. Phys. Chem. 82 (1966) 138–141.
[44] C.S. Turchi, D.F. Ollis, J. Catal. 122 (1990) 178–192.
[45] J.H. Baxendale, J.A. Wilson, Trans. Faraday Soc. 53 (1957) 344–356.
[46] G.V. Buxton, C.L. Greenstock, W.P. Helman, A.B. Ross, J. Phys. Chem. Ref. Data 17 (1988) 513–886.
[47] M. Sui, L. Sheng, K. Lu, F. Tian, Appl. Catal. B: Environ. 96 (2010) 94–100.

[48] M.D. Gurol, S. Nekouinaini, J. Water Pollut. Control Feder. 57 (1985) 235–240.
[49] C. Tizaoui, N.M. Grima, M.Z. Derdar, Chem. Eng. Sci. 64 (2009) 4375–4382.
[50] P. Palominos, J. Freer, M.A. Mondaca, H.D. Mansilla, J. Photochem. Photobiol. A: Chem. 193 (2008) 139–145.
[51] P.S. Bailey, Chem. Rev. 58 (1958) 925–1010.
[52] P. Calza, V.A. Sakkas, C. Medana, C. Baiocchi, A. Dimos, E. Pelizzetti, T. Albanis, Appl. Catal. B: Environ. 67 (2006) 197–205.
[53] D. Vogna, R. Marotta, A. Napolitano, R. Andreozzi, M. d'Ischia, Water Res. 38 (2004) 414–422.
[54] E.D. Black, E. Hayon, J. Phys. Chem. 74 (1970) 3199–3203.
[55] F.J. Beltrán, Ozone Reaction Kinetics for Water and Wastewater Systems, Lewis Publishers, Boca Ratón, FL, 2004.
[56] A.C. Pierpoint, C.J. Hapeman, A. Torrents, J. Agric. Food Chem. 49 (2001) 3827–3832.
[57] Farhataziz, A.B. Ross, Nat. Std. Ref Data Ser. U. S. Nat. Bur. of Std. (1977) 59.
[58] W.T.M. Adenauer, M. Callewaert, I. Nopens, J. Cromphout, R. Vanhoucke, A. Dumoulin, P. Dejans, S.W.H. van Hulle, Chem. Eng. J. 157 (2010) 551–557.